Simulating $t\bar{t}$ events with additional jets at the LHC

Stefan Richter

PhD transfer report · University College London · August 26, 2014
Supervisors: Emily Nurse, Keith Hamilton

Abstract

The ATLAS and CMS collaborations have recently studied top quark production with additional jet activity in proton-proton collisions at $\sqrt{s} = 7$ and 8 TeV and found some disagreement between the experimental data and the predictions of state-of-the-art Monte Carlo event generators. We studied the effect of different setups of the event generator combination Powheg + Pythia 8 on the rapidity-dependent rates of additional jets, and tried to choose settings such that a better description of the data was achieved. The agreement between data and simulation could be improved significantly by damping resummation of soft-gluon effects in Powheg in cases where the emitted parton with the greatest transverse momentum has an absolute rapidity of more than 1.5 units in the laboratory frame. We also validated the matching of Pythia 8 parton showers to Powheg matrix elements in the case of $t\bar{t}$ events at the LHC.

Contents

1 Introduction: tops, jets, and gaps

Top quarks are the heaviest known elementary particles. In proton-proton collisions at the Large Hadron Collider (LHC), they are mainly produced as top-antitop quark pairs ($t\bar{t}$). The $t\bar{t}$ production cross section[1] is around 160 (230, 880) pb at a proton collision energy of $\sqrt{s}$ = 7 (8, 14) TeV, or around 20 (30, 120) times larger than at the Tevatron, the collider at which the top quark was discovered, earning the LHC the title of a *top factory*. Because of its high mass, the top quark plays a special role in the study of the standard model of particle physics and searches for physics beyond it. It makes the top quark couple very strongly to Higgs bosons and $t\bar{t}$ production a prototype process for the production of new massive particles, whereas the vast majority of hadron collisions produce only very low-mass systems. Experimentally, $t\bar{t}$ events have a rich phenomenology due to the the fact that top quarks practically always decay to W bosons, which in turn decay to many different possible final states. Almost all of the different physical objects in terms of which analysis is done at the LHC can be produced in $t\bar{t}$ events: electrons, muons, tau leptons, gluon and light-flavour jets, heavy-flavour-tagged jets, and missing transverse energy due to neutrinos. Only energetic photons are rare. This multitude of final states and the high top quark mass leading to large transverse momenta of the decay products mean that $t\bar{t}$ events constitute a background in many searches for new physics, prompting the expression "new physics hides under the top." New physics is also searched for in decays of the top quark, such as the hypothetical $t \to H^+b$, where H^+ is a charged Higgs boson. The mass of the top quark lies well above that of the W boson, meaning that top quarks decay weakly before having time to form hadrons.[2] This makes the top quark the only known laboratory for studying quarks decaying outside of hadrons.

For the above reasons and others, it is important to understand $t\bar{t}$ events with high quantitative precision. There is little hope of discovering new phenomena without being able to describe their background of known physics. At the same time, the theoretical description of $t\bar{t}$ events is relatively complex, due to the large number of contributing quantum chromodynamics (QCD) Feynman diagrams and consequently many possible colour flows, as well as the massiveness of the top quark introducing an additional non-negligible mass scale into the calculation.

A recent study [1] by the ATLAS collaboration measured the activity of additional jets in $t\bar{t}$ events, i.e. jets not coming from the decays of the top quarks. Understanding additional jets is important because they change the event topology, to which analysis strategies may need to be adapted if $t\bar{t}$ processes are the signal or a background. In addition, their measurement constitutes a precision test of the standard model and the approximations used to make predictions. Additional jets could be initiated by energetic QCD radiation from the partons participating in the hard process, or the scattering of additional partons in the colliding protons (multiparton interactions, MPI).

The ATLAS study selected $t\bar{t}$ events in the dilepton decay channel in proton-proton collisions at $\sqrt{s}$ = 7 TeV. Tau leptons decay to a number of final states before being detected, so only electrons and muons and their antiparticles were considered leptons in this context, as is common in collider physics. Jets were constructed using the anti-$k_\perp$ algorithm [6] with radius parameter $R = 0.4$ in η-ϕ space and required to have $p_\perp > 25$ GeV and $|\eta| < 2.4$. Two identified b-jets were required. The additional jet activity was studied by counting events with and without gaps. A gap is a range in rapidity in which there are no additional jets. Two kinds of gaps were considered separately in the analysis. Events were defined to have a gap if there were no additional jets with transverse momentum larger than a threshold value Q_0 in the given rapidity range (1$^{\text{st}}$ kind) or if the scalar sum of the transverse momenta of all additional jets in the given rapidity range was below Q_{sum} (2$^{\text{nd}}$ kind). Gaps were counted in three exclusive rapidity ranges, $|y| < 0.8$, $0.8 < |y| < 1.5$, and $1.5 < |y| < 2.1$, as well as the inclusive range $|y| < 2.1$. The number of $t\bar{t}$ events with a gap divided by the total number of observed $t\bar{t}$ events is called the gap fraction f_{gap}. Differential gap fractions as a function of Q_0 or Q_{sum}, respectively, were measured in each of the four rapidity regions. The results were corrected for detector effects. The gap fractions increase monotonically as the threshold value increases and approach unity: at some very high transverse momentum defined by phase space boundaries it is no longer possible to produce jets,

[1] Here calculated using the web application at `http://www.lpthe.jussieu.fr/~cacciari/ttbar` implementing the calculation in ref. [4].

[2] The fast decay is the result of a large available decay phase space, as well as strong Yukawa-like coupling of the top quark to longitudinally polarised W-bosons leading to an effectively semi-weak decay [5].

so all events have a gap there. They can be thought of as cumulative probability density functions: at each threshold transverse momentum, they show the probability of not having a jet harder than this transverse momentum in the veto region.

It was found that the experimentally measured gap fractions are not described to within experimental uncertainty (systematic and statistical) by state-of-the-art Monte Carlo (MC) event generators, namely the combinations of MC@NLO + Herwig++ and Powheg + Pythia 8.

In this study, we focus on the combination Powheg + Pythia 8, which tends to predict too many jets and hence too low gap fractions. We study the effect of different generator settings on the gap fractions and try to "tune" them to achieve a better description of the data. We also validate the combining (*matching*) of Pythia 8 parton showers with Powheg NLO matrix elements for $\mathrm{t\bar{t}}$ events. We try to understand the theoretical uncertainties related to the different settings and assess their numerical importance. The overall goal is to improve the understanding and description of additional jet rates and spectra in the so important $\mathrm{t\bar{t}}$ events.

Gap fractions in $\mathrm{t\bar{t}}$ events have also been measured by the CMS collaboration [2, 3]. Data/MC discrepancy similar to that in the ATLAS measurement is observed for Powheg + Pythia 8. This independent confirmation makes it less likely that the disagreement is due to experimental effects that have not been taken into account correctly.

2 Improving Powheg + Pythia 8 simulation of $\mathrm{t\bar{t}}$ + jets

In the simulation of $\mathrm{t\bar{t}}$ events with Powheg + Pythia 8, Powheg generates the hard processes of the form $\mathrm{gg}/q\bar{q} \rightarrow \mathrm{t\bar{t}}$ at next-to-leading order accuracy in α_s, as well as the emission of the additional gluon with the highest transverse momentum ("hardest"). Pythia 8 reads the Powheg output dresses the hard process with initial- and final-state radiation using the parton shower formalism, recombines the soft partons from the shower to hadrons, lets short-lived particles decay, and generates multiparton interactions. Among many other parameters related to all of these actions, the user has control over whether Powheg or Pythia 8 generates the decays of the top quarks as well as how Pythia 8 matches its parton showers and multiparton interactions to the Powheg input. The reason for using Powheg is to get the better accuracy it achieves, which improves in particular the normalisation of the $\mathrm{t\bar{t}}$ production cross section and the description of the hardest QCD radiation in the event. Pythia 8 is used achieve a complete description of events to compare to data.

2.1 NLO QCD matrix elements and parton showers

Parton shower. NLO $\mathrm{t\bar{t}}$ matrix elements have two or three coloured partons in the final state, but what is observed with the ATLAS detector are large numbers of uncoloured particles. To get from the matrix element to the physical final state, one first takes into account that coloured partons radiate in a changing colour field, much like electrically charged particles emitting Bremsstrahlung. Since both quarks and gluons carry colour charge, the radiated partons themselves emit further partons, leading to a cascade of coloured particles forming around the direction of each original, energetic parton. The important higher-order corrections to the matrix element come from those branchings in the cascade where the opening angle between the two produced partons is very small, or one of them is a low-energy gluon. In the limit where the branching is nearly collinear, the matrix element factorises, so that each parton in the event at a given time can be treated as branching independently of other partons and the process that produced it. The parton shower formalism is a Monte Carlo approach to implementing approximate corrections to all orders in the strong coupling constant based on the approximation where branchings are nearly collinear. In the parton shower, the branching cross sections of a parton are proportional to powers of logarithms L of the form

$$L = \log\left(\frac{\text{scale of previous branching}}{\text{scale of current branching}}\right), \tag{1}$$

where the scale could be e.g. the relative transverse momentum between the partons after the branching[3], which is small when they are collinear and/or one is soft, making L large. On the other hand, if the scale of the current branching is not much smaller than that of the previous, L remains of order 1 and the branching is less probable. Since the parton shower only aims to describe the logarithmically enhanced contributions, an ordering in scale is enforced, such that the evolution is from higher to consecutively lower scales. It is terminated at around 1 GeV, as the strong coupling constant becomes large below this value and the perturbative description breaks down. At this point, the partons are combined into hadrons according to a phenomenological hadronisation model. Branching steps with probability proportional to two powers of L for each power of α_s are called leading-logarithmic (LL) contributions, those with one power of L next-to-leading-logarithmic (NLL). LL contributions come from branchings that are both soft *and* collinear, NLL contributions from those that are either soft *or* collinear.

The parton shower is used to generate radiation off the final-state partons (FSR), but also initial-state radiation (ISR) off the incoming partons. Partons emitted as ISR then go on to form their own FSR cascades. Pythia 8 accommodates ISR and FSR emissions as well as multiparton interactions in a single sequence of decreasing transverse momentum [7]. In $\mathrm{t\bar{t}}$ events, practically all radiation from the hard process is ISR. There is no collinear enhancement associated with radiation off the top quarks due to their mass, while the soft-enhanced radiation off them is independent of their direction and can be treated as ISR.

Pythia 8 parton shower. If Pythia 8 is used on its own, the final-state kinematics of the hard process are generated first, according to the LO cross section

$$\mathrm{d}\sigma_{\mathrm{LO}} = \mathcal{B}(\Phi_n)\,\mathrm{d}\Phi_n, \tag{2}$$

where the $\mathcal{B}$ is the squared sum of leading-order matrix elements after averaging and summing over spin and colour, and Φ_n stands for the n-particle phase space describing the final-state kinematics, but also including momentum fractions of the incoming partons.

Then the parton shower generates emissions from the partons. Considering only radiation from the incoming partons 1 and 2, the kinematics of the first emission, with transverse momentum $p_\perp$, are generated according to

$$\mathrm{d}\sigma^{\mathrm{hardest}}_{\mathrm{py8}} = \mathrm{d}\sigma_{\mathrm{LO}}\;\Delta_1(p_\perp)\Delta_2(p_\perp)\;\alpha_s\left[P_{1\to jk}\;\mathrm{d}\Phi_{\mathrm{rad},1} + P_{2\to jk}\;\mathrm{d}\Phi_{\mathrm{rad},2}\right] \tag{3}$$

where:

- $\Delta_i(p_\perp)$ is called a *Sudakov form factor* and gives the probability that parton i does not branch with transverse momentum above $p_\perp$,
- $P_{i\to jk}$ is a universal splitting function, proportional to the probability of parton flavour i splitting to parton flavours j and k,
- $\mathrm{d}\Phi_{\mathrm{rad},i}$ is the phase space of the hardest emission from parton i.

Thus $\alpha_s P_{i\to jk}\mathrm{d}\Phi_{\mathrm{rad},i}$ is the probability of an emission into phase space element $\mathrm{d}\Phi_{\mathrm{rad},i}$. In the same approximation as the rest of the parton shower, the Sudakov form factor is given by

$$\Delta_i(p_\perp) = e^{-\int \alpha_s P_{i\to jk}\,F(\Phi_{\mathrm{rad},i})\,\mathrm{d}\Phi_{\mathrm{rad},i}}, \tag{4}$$

where the integration over transverse momentum in $\mathrm{d}\Phi_{\mathrm{rad},i}$ is from $p_\perp$ up to the scale of the hard process. It is implied that all possible post-branching flavours j, k are summed over.

The factor $F(\Phi_{\mathrm{rad}})$ depends on whether the emission is from the initial state of the hard process or not. ISR means that the parton with momentum fraction x' taken from the proton parton density function (PDF) is no longer the same as the one entering the hard scattering with momentum fraction x. For this reason, the Sudakov form factor for ISR includes a ratio of momentum fractions and PDFs

[3]The choice of scale is not unambiguous, e.g. the invariant mass of the produced partons might also be used. Pythia 8 and Powheg use transverse momentum.

$f_i(x, Q^2)$ before and after the branching. Using the ISR notations

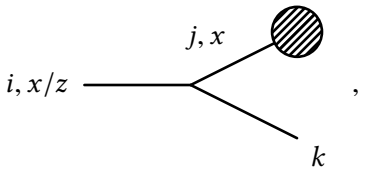

with the blob representing the rest of the evolution up to and including the hard process, we have

$$F(\Phi_{\text{rad}}) = \begin{cases} \frac{x/z}{x} \frac{f_i(x/z;p_\perp^2)}{f_j(x;p_\perp^2)} & \text{if ISR,} \\ 1 & \text{if FSR.} \end{cases} \tag{5}$$

Subsequent emissions with consecutively lower transverse momentum are then attached to the new final state iteratively. The transverse momentum integration in the Sudakov form factor is from that of the current branching up to that of the previous one. The evolution is continued all the way down to the hadronisation scale, 0.5 GeV in the case of Pythia 8. In this way, the parton shower resums[4] the dominant parts of higher-order corrections to all orders in the strong coupling constant.

Powheg. Powheg [8–10] is a general method and framework for generating matrix-element level events at next-to-leading order (NLO) accuracy in the relevant coupling constant(s). We generated top quark events at NLO in the strong coupling constant α_s with the Powheg-hvq (for *heavy quark*) generator [11], here simply referred to as Powheg for brevity.

While the leading-order (LO) Feynman diagrams of $t\bar{t}$ production are tree-level, contributing terms of order α_s^2 to the cross section, NLO (α_s^3) terms include both diagrams with loops of virtual partons and diagrams featuring the emission of a real additional parton, corresponding to different final states with different phase spaces. The virtual-correction amplitudes contain one more power of α_s than the real-emission amplitudes. At NLO, they only enter through their interference with the LO amplitude. Contributions to the NLO cross section—after spin and colour sums and averages and including an appropriate flux factor—proportional to

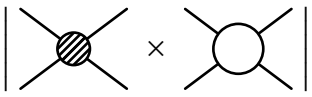

are denoted $\mathcal{V}$ (for *virtual correction*) and terms proportional to

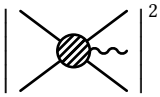

are denoted $\mathcal{R}$ (for *real emission*). The NLO cross section can be written schematically as

$$\mathrm{d}\sigma_{\text{NLO}} = [\mathcal{B}(\Phi_n) + \alpha_s \mathcal{V}(\Phi_n)]\, \mathrm{d}\Phi_n + \alpha_s \mathcal{R}(\Phi_{n+1}) \mathrm{d}\Phi_{n+1}. \tag{6}$$

The $(n + 1)$-particle phase space factorises into the underlying n-particle configuration (including a suitable Jacobian) and the radiation phase space, $\mathrm{d}\Phi_{n+1} \to \mathrm{d}\Phi_n \mathrm{d}\Phi_{\text{rad}}$.

Just as in the LO case, Powheg first generates the hard n-particle configuration, but now at NLO accuracy according to the cross section

$$\mathrm{d}\sigma_{\text{NLO},\, n} = \overline{\mathcal{B}}(\Phi_n)\ \mathrm{d}\Phi_n, \tag{7}$$

where

$$\overline{\mathcal{B}}(\Phi_n) = \mathcal{B}(\Phi_n) + \alpha_s \mathcal{V}(\Phi_n) + \int \alpha_s \mathcal{R}(\Phi_n, \Phi_{\text{rad}})\ \mathrm{d}\Phi_{\text{rad}}. \tag{8}$$

[4]Resummation: making a perturbative expansion, calculating its terms in some approximation, and summing them up to all orders. It is neither an exact nor a fixed-order calculation.

It then generates one real emission on top of the n-particle configuration, which is constructed to be the emission with the highest transverse momentum, harder than all further emissions that will subsequently be generated by the parton shower. In NLO calculations, cancellation of infrared divergences between real-emission and virtual correction cross sections happens in the regions of phase space where some partons are soft and/or collinear to each other. This is precisely the region of phase space where higher-order corrections are large. One would like to use the same approach as in a parton shower in these regions in order to resum the dominant corrections to all orders in the strong coupling constant. In Powheg, this is achieved by including a modified Sudakov form factor Δ_{pwg} in the cross section. The form factor is different from the parton shower case in that it includes the full radiation cross section instead of approximate splitting functions,

$$\Delta_{\text{pwg}}(p_\perp) = e^{-\int \alpha_s \frac{\mathcal{R}(\Phi_n,\Phi_{\text{rad}})}{\mathcal{B}(\Phi_n)} F(\Phi_{\text{rad}})\, \mathrm{d}\Phi_{\text{rad}}}, \tag{9}$$

where $p_\perp$ is the transverse momentum of the hardest emission and the integration over transverse momentum in $\mathrm{d}\Phi_{\text{rad}}$ is from $p_\perp$ up to the scale of the hard process. The full cross section according to which the hardest emission is generated is then

$$\mathrm{d}\sigma^{\text{hardest}}_{\text{pwg}} = \mathrm{d}\sigma_{\text{NLO},\,n}\, \Delta_{\text{pwg}}(p_\perp)\, \alpha_s \frac{\mathcal{R}(\Phi_n,\Phi_{\text{rad}})}{\mathcal{B}(\Phi_n)}\, \mathrm{d}\Phi_{\text{rad}}. \tag{10}$$

This cross section contains only one term and a single Sudakov form factor, whereas the parton shower description in equation (3) had two terms and a product of two form factors. The reason is that contributions due to each emitting parton are separated in the parton shower, while the NLO calculation includes interference. The single form factor infused with a NLO matrix element in Powheg corresponds to the product of the two form factors in the parton shower case above. They too can be written as a single factor by summing the exponents.

If one had not included the Sudakov form factor, the cross section in equation (10) would diverge in the limit where the transverse momentum $p_\perp$ of the emission becomes very small. A hand-waving physical explanation of why the Sudakov form factor prevents this is that it provides a more accurate description of nature by implementing the important parts of corrections to all orders, and nature is free of divergences. Mathematically, the pure NLO cross section diverges as $1/p_\perp^2$, whereas the leading behaviour of the Sudakov form factor is as $e^{-\alpha_s \log^2(Q^2/p_\perp^2)}$, so that the product of the two remains finite.

In the limit where $p_\perp$ is very low, the ratio $\mathcal{R}/\mathcal{B}$ becomes equal to the sum of splitting functions $P_{i\to jk}$ for each of the partons in the n-particle event and one recovers the parton shower description of equation (3). On the other hand, if $p_\perp$ is high, the Sudakov form factor is of order 1 and one recovers the pure NLO matrix element description. In addition, when integrating the Powheg cross section over the radiation phase space, one recovers the NLO cross section of the underlying n-particle process,

$$\int \frac{\mathrm{d}\sigma^{\text{hardest}}_{\text{pwg}}}{\mathrm{d}\Phi_{\text{rad}}}\, \mathrm{d}\Phi_{\text{rad}} = \mathrm{d}\sigma_{\text{NLO},\,n}, \tag{11}$$

so inclusive quantities calculated in Powheg-generated events have next-to-leading-order accuracy. A formal proof that arbitrary infrared-safe observables are described at NLO accuracy in Powheg can be found in ref. [9].

Combining Powheg and Pythia 8. The problem of matching a parton shower to an NLO matrix element is essentially one of avoiding over- or undercounting of emissions. Powheg has already performed the evolution from the scale of the hard process to the scale of the hardest additional emission, therefore Pythia 8 should not generate radiation between these scales so as not to overcount emissions. The same is true for virtual corrections, which the parton shower also resums approximately. Equally, if the parton shower does not generate emissions starting from the hardest emission scale downwards, but some lower scale, this introduces undercounting. From this perspective, the correct way to match Powheg and Pythia 8 is to make sure that no Pythia 8 parton shower emissions are harder than the Powheg emission.

Powheg is particularly suited for use with Pythia 8, because the latter generates parton showers ordered in transverse momentum. The matching is then basically as easy as letting the shower evolution start at the $p_\perp$ of the hardest emission generated by Powheg. Matters are somewhat complicated by the fact that both Pythia 8 and Powheg compute transverse momentum in a collinear approximation and use a different definition to do so (see section A). The definitions agree in the collinear limit, but not away from it. In order to get more control over which $p_\perp$ definition is used and other aspects of the matching, one can use a veto algorithm for the parton shower:

1. Compute scale of the Powheg emission using some $p_\perp$ definition
2. Set shower starting scale to some very high value (e.g. $\sqrt{s}$)
3. Generate next parton shower emission and compute its scale using some $p_\perp$ definition
4. Veto emission if its scale is larger than the scale of the Powheg emission, otherwise keep it
5. Go to 3., continuing the evolution from the scale of the last emission (vetoed or kept)

Such an algorithm is implemented in the Pythia 8 example program `main31`, and the name `main31` has become all but synonymous with this type of matching in the experimental community.

The `main31` program has a large number of customisable settings related to how the vetoing scale and the scales of emissions are computed, including some rather experimental ones. Appendix A is devoted to explaining the different settings. At this point, we will limit ourselves to remarking that the default settings, corresponding to our baseline scenario, describe the of gap fraction data best. The difference between using the Powheg or Pythia 8 $p_\perp$ definition is very small.

2.2 Gap fractions and baseline scenario

The gap fraction distributions measured by ATLAS have been made available in the Rivet framework [12] (analysis identifier `ATLAS_2012_I1094568`), where they can be directly compared to MC predictions. This allowed us to test various settings.

Baseline scenario. To make the study more systematic, we defined the following *baseline scenario* in terms of a generator setup to compare against. Powheg-hvq was used to generate matrix-element-level $\mathrm{t\bar{t}}$ events and decays of the top quarks to electrons or muons ($\mathrm{t} \to \mathrm{bW} \to \mathrm{b}\ell\nu$), after which the events where processed with Pythia 8 for parton showering, multiparton interactions, electroweak radiation, and hadronisation. Powheg and Pythia 8 were matched using the unmodified `main31` program with default configuration settings (given in appendix A). Except for some parameters in Pythia 8 influenced by `main31`, both generators use all their respective default settings, such as choices of coupling constants, particle masses, and parton density function sets. Where generator defaults are not defined, ATLAS defaults are used, which correspond closely to the current world averages [13].

Experimentally measured gap fractions along with our baseline MC prediction are shown in figures 1 and 2. The statistical uncertainty of the data points is indicated by error bars, while the yellow uncertainty band in the ratio plot shows the statistical and systematic uncertainty of the measurements added in quadrature. In some figures, the statistical uncertainty of the MC prediction is shown as error bars. Surprisingly, re-generating events with identical settings leads to fluctuations that are much larger than the statistical uncertainty would suggest, so the error bars on the MC prediction are unrealistically small. The reason for this is still unknown.

The degree of agreement of the baseline MC prediction with the ATLAS data in each rapidity region is sketched in figure 3. The disagreement is significant only in the most forward rapidity region. In the figure, the mass of the additional jets has been considered negligible, in which case their rapidity becomes equal to their pseudorapidity η, which is unambiguously related to the scattering angle θ by the relation $\eta = -\log(\tan(\theta/2))$. This allows us to represent rapidity regions as angular regions. It is found that the data/MC agreement is good in some rapidity regions, and poor in the most forward region, $1.5 < |y| < 2.1$. The challenge will be to find a way to improve the modelling particularly in this region without breaking it in the regions where the baseline scenario performs well.

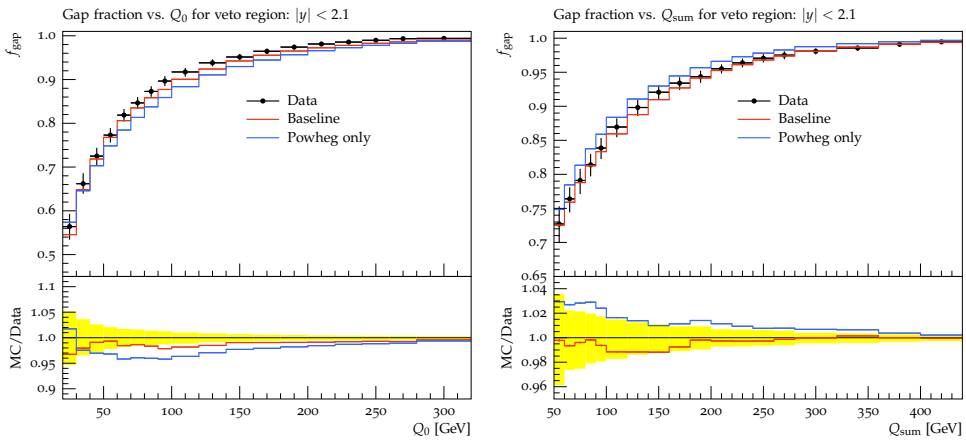

Figure 1: Baseline MC prediction as well as prediction of Powheg NLO matrix elements alone for gap fractions in the inclusive rapidity region.

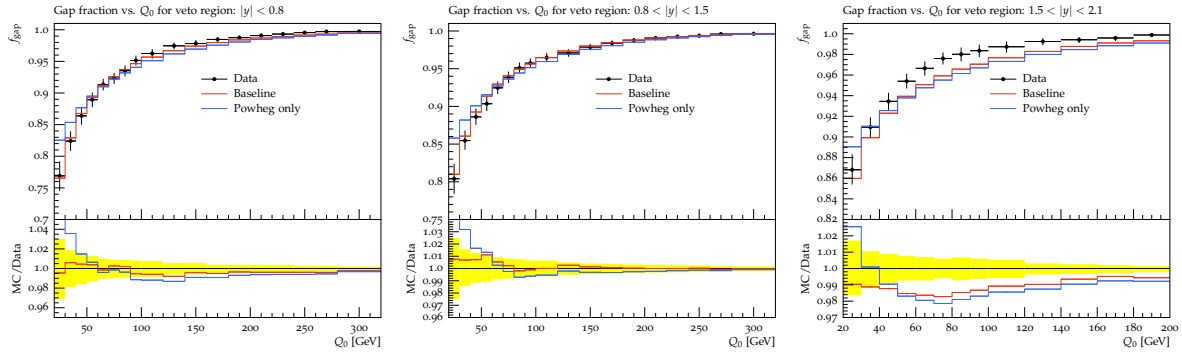

Figure 2: Baseline MC prediction as well as prediction of Powheg NLO matrix elements alone for Q_0 gap fractions in the exclusive rapidity regions. Q_{sum} gap fractions are not shown, because their level of data/MC agreement is similar to that of the Q_0 fractions in the same region.

The gap fractions are a tricky observable in that they are sensitive in a highly non-trivial way to many different phenomena and parameters, as we will explore below. The Q_0 gap fractions are sensitive to the hardest additional jet *in the considered rapidity region*, which is not necessarily the hardest additional jet in the entire event. Modelling of gap fractions with narrow veto regions therefore means relying heavily on the parton shower formalism to get jet distributions right, despite its approximate nature. In addition, the exclusive gap fractions do not 'add up' trivially to give the inclusive ones.

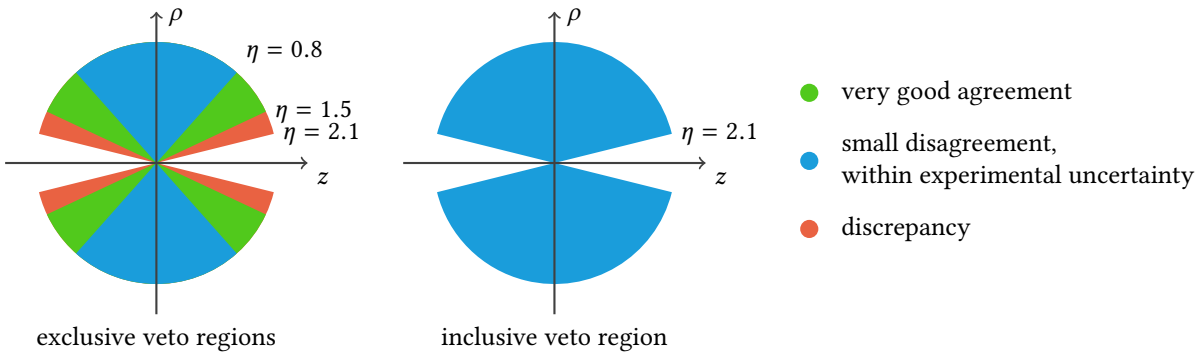

Figure 3: Agreement of the baseline MC prediction with the data in the different veto rapidity regions, visualised as a longitudinal section through the detector. Massless jets have been assumed, in which case $y = \eta$. Proton beams move along $\pm z$, collisions occur at the origin, and ρ is the radial distance from the beams.

2.3 Contribution of Pythia 8

The first thing we checked is to what extent the gap fractions in simulation are determined by Powheg and to what extent by Pythia 8.[5] The comparison in the inclusive rapidity region is shown in figure 1. It can be seen that Powheg alone gives a good approximate description of both Q_0 and Q_{sum} gap fractions, to within about 4% of the experimental values in the inclusive rapidity region. This demonstrates how nicely a direct connection can be made between between individual hard partons and jets consisting of tens or even hundreds of particles. Differences between the gap fractions with and without Pythia 8 are observed for both Q_0 and Q_{sum} gap fractions, with the latter differences being larger. We will show below that hadronisation and multiparton interactions have very little impact on the gap fractions, so we can consider the differences to be almost entirely due to parton showering. It is clear from figures 1 and 2 that including parton showering improves the gap fraction prediction.

In Q_0 gap fractions, turning off parton showering leads to more gaps at the very low-momentum end of the spectrum. This is likely due to configurations where the hardest emission generated by Powheg falls outside of the gap rapidity range, but a second and sufficiently hard ISR emission generated by Pythia 8 might make the event gapless. At higher Q_0, there are less gaps without Pythia 8. The probable cause is that parton shower emissions slightly deplete the energy of the jet initiated by the hardest emission, since a part of the radiation ends up outside of the jet cone. The process is illustrated in figure 4 and shown in event generation in figure 5. Thus the parton shower shifts gaps from higher to lower Q_0.

(a) (b)

Figure 4: Parton-level jet clustering without parton shower (a) and with parton shower (b). In the latter case, the transverse momentum of the jet is depleted by emissions ending up outside of the jet cone.

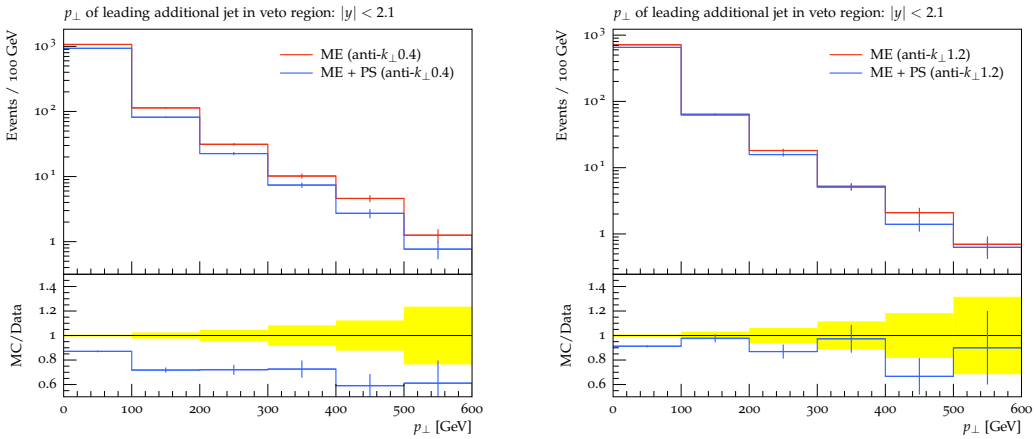

(a) (b)

Figure 5: Transverse momentum of the leading additional jet with rapidity $|y| < 2.1$ using a jet radius of 0.4 (a) or 1.2 (b). Both the Powheg matrix element (ME) prediction and the prediction including the parton shower (PS) are shown. A larger jet radius captures more radiation and thereby leads to a smaller difference between the two. Note that a larger jet radius leads to different numbers of additional jets even at the matrix element level by making it more probable that the hardest emission is clustered into the same jet with one of the beauty quarks from top quark decay.

In Q_{sum} gap fractions, where all additional jets are considered together, the lack of additional radiation

[5] This requires minimal modification of the ATLAS Rivet analysis for measuring the gap fractions, such that it can operate on parton-level input rather than hadrons. The modified source code and instructions can be requested from the author.

from Pythia 8 leads to higher gap fractions, because no additional jets due to further initial-state radiation or multiparton interactions are present. Q_{sum} gap fractions are directly sensitive to emissions beyond the hardest, and are always decreased when parton showering is performed.

In the Powheg-level events, the only possible source of an additional jet is the hardest emission and the prediction for Q_0 and Q_{sum} gap fractions is identical. At this level, the distribution of gap fractions has a similar interpretation as the Sudakov form factor: both describe the probability of not having an emission harder than Q_0 or $p_\perp$, respectively. The difference is that the hardest emission falling within a certain rapidity range is considered for the gap fractions, which is not necessarily the hardest emission in the entire event. As we have seen, the situation becomes more complicated when further emissions are included, since these can deplete the energy of the jets associated with the hardest partons and may give rise to additional jets.

Hadronisation effects. The effect of the hadronisation model on the gap fractions is shown in figure 6. It is very small and can be considered negligible for our purposes. Its direction is the same in all gap fraction distributions, namely to increase gap fractions at low Q_0 or Q_{sum}. The reason is probably that hadrons may end up outside of jets, thus depleting their transverse momentum, just like parton shower emissions. The effect may be weaker in harder jets, where the boosting effect causes them to be more collimated. This would explain why the low-$p_\perp$ end of the gap fraction spectrum is affected more.

The parton-level final state analysed here is not physical, but the gap fractions should still be, since the anti-$k_\perp$ algorithm used to construct the jets is infrared- and collinear-safe (i.e. not sensitive to additional partons with very little energy and the splitting of one parton into two moving in the same direction).

Multiparton interactions. Multiparton interactions happen mostly at low scales and mainly produce additional hadrons with low transverse momentum in the event. These may be reconstructed as mostly soft jets, but also end up inside the jets associated with the hard process, increasing their measured transverse momentum. The distribution of energy deposits due to MPI is on average approximately even in η and ϕ. Therefore, the average additional energy of a jet due to MPI is proportional to the jet area in η-ϕ space, i.e. proportional to the square of its radius R. The analysis uses relatively narrow jets with $R = 0.4$. Therefore, the effect of MPI on gap fractions is expected to be small. Event generation confirms this, as is shown in figure 6. Understanding the effect of turning MPI on and off in detail is complicated by the interleaving of MPI with the parton shower in Pythia 8. MPI 'steal' energy from the parton shower, meaning that when MPI are turned off, the hard jets may lose less transverse momentum to radiation out of the jet cone.

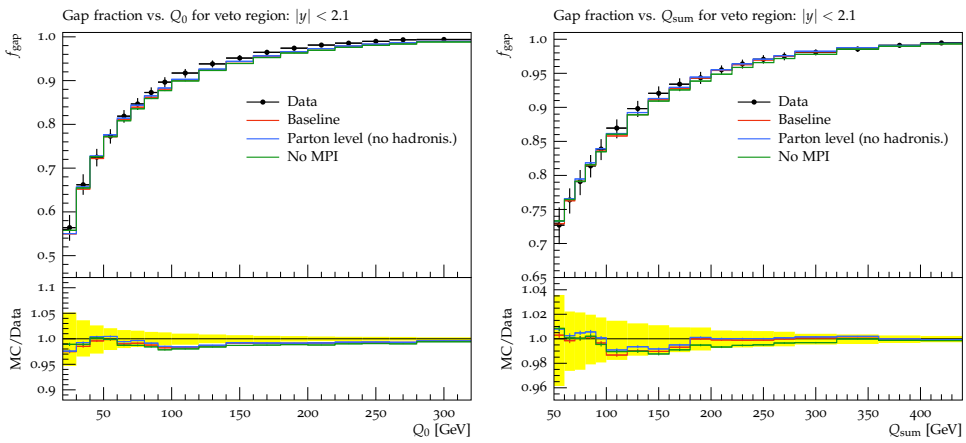

Figure 6: Effects of hadronisation and multiparton interactions.

Matching scale. How sensitive are the gap fractions to variations in the matching scale of Powheg and Pythia 8, i.e. the scale above which parton shower emissions are vetoed? Increasing the matching scale introduces overcounting, and reducing it undercounting of emissions. If the starting scale of the

shower is increased, this changes both the integrand and the upper limit of the transverse momentum integration in the Sudakov form factor of the parton shower, leading to more emissions at large transverse momentum. Lowering the starting scale correspondingly makes emissions at large transverse momentum less probable. Formally, the variation introduces logarithmically enhanced terms proportional to $L\alpha_s$ in the exponent of the Sudakov form factor and thus is a NLL effect. Since the formal accuracy of the shower is only at the LL level (though some NLL effects are included), it should be permissible to vary the matching scale by a factor not much larger than unity, say 2. On the other hand, raising the matching scale may lead to the parton shower producing harder emissions than Powheg, which is not desirable: the leading behaviour should be determined by the most accurate calculation, not a cruder approximation.

Figure 7 shows how the effect of such variations on the gap fractions. An increased matching scale leads to lower gap fractions (more jets) and a decreased scale to higher gap fractions (less jets). Qualitatively, the results are as expected, but their numerical size is surprisingly large given that they are formally a modest effect. As an observable, the gap fraction seems to be very sensitive to the matching scale and may therefore be a useful in validating the matching. Even lowering the matching scale by a factor of 0.5, thus introducing substantial undercounting in the parton shower, does not raise gap fractions sufficiently to give agreement in the problematic rapidity region (1.5–2.1).

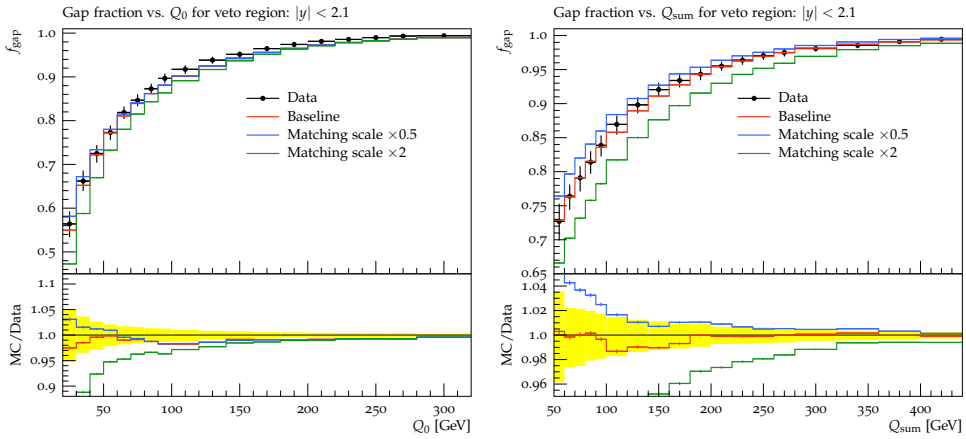

Figure 7: Changing the matching scale of the parton shower.

2.4 Top quark decay

Top quarks decay to a W boson and a down-type quark with a branching fraction greater than 99.9% [13]. We are interested in events where both W bosons decay to $\ell\nu_\ell$, which constitute about 5% of all $t\bar{t}$ events.[6] A comparison of samples with dileptonic as well as all possible top decays, generated by Powheg or Pythia 8, is shown in figure 8. Powheg-generated decays take into accound the top quark polarisation. No significant difference between the different decay simulations is observed.

2.5 Parton density functions

The PDFs influence the generation of the hard process, multiparton interactions, and initial-state radiation. For our choice of generators, the PDF set chosen in Powheg influences the hard process and the first ISR emission, while that chosen in Pythia 8 influences any subsequent shower emissions after the hardest, as well as multiparton interactions. The rate of ISR emissions depends on the ratio of PDFs evaluated at two momentum fractions (equation (5)), which appears in the Sudakov form factor for ISR, equations (4) and (9). This is interesting for our present study, because PDFs depend on the rapidity of the emitted parton, which is given by the momentum fractions x_1 and x_2 of the incoming partons.

[6] Calculated assuming lepton universality, vanishing masses of all leptons and quarks up to the beauty quark, and vanishing off-diagonal elements in the CKM quark flavour mixing matrix.

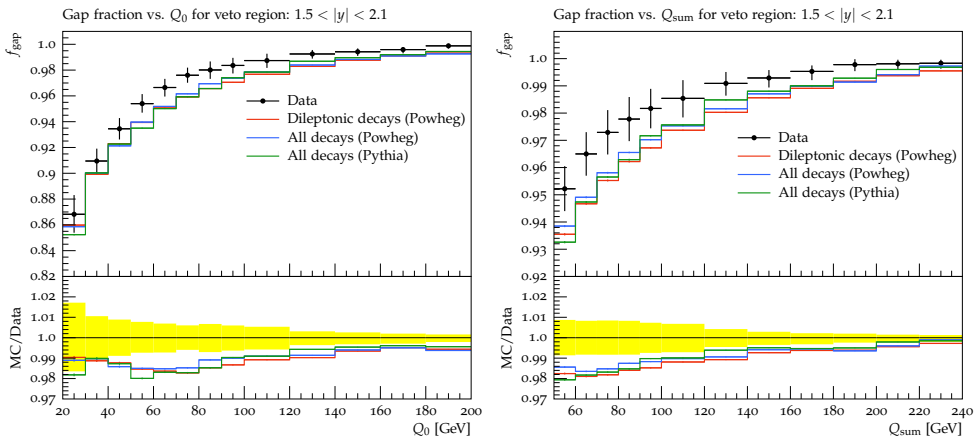

Figure 8: Different top quark decays simulated with different generators.

Since the observed data/MC disagreement is different in different rapidity regions, PDF variations might improve the agreement in the problematic region without spoiling it in the well-described regions.

PDFs evolving at different orders in α_s have been constructed. There are some qualitative differences between LO and NLO PDFs. Powheg requires NLO PDFs for consistency, but these are not well suited for the LO shower and MPI models in Pythia 8 [14], so it is erroneous to think that NLO PDFs are always superior to LO ones. NLO PDFs can assume negative values and tend to have smaller gluon contributions at low x, which is compensated for by positive corrections in the NLO matrix elements [14]. Another important difference between different PDF sets, in particular in LO vs. NLO, is the value and order of running of α_s. Powheg, but not Pythia 8, takes the value of $\alpha_s(M_Z)$ from the PDF. Using NLO PDFs in Powheg and LO PDFs in Pythia 8 is probably the best alternative [15].

Set *(default choice in…)*	PDF evolution	Minimum x value	Q^2 range (GeV^2)	$\alpha_s(M_Z)$ value	α_s running order
CTEQ6M [16] *(Powheg-hvq)*	NLO	10^{-6}	1.69 to 10^8	0.1179	NLO
CT10 [17]	NLO	10^{-8}	1.69 to 10^{10}	0.118	NLO
HERAPDF 1.5 NLO [18]	NLO	10^{-8}	1.0 to 10^9	0.1176	NLO
MRST2004 NLO [19]	NLO	10^{-5}	1.25 to 10^7	0.1205	NLO
MSTW2008 NLO [20]	NLO	10^{-6}	1.0 to 10^9	0.12018	NLO
CTEQ5L [21] *(Pythia 8)*	LO	10^{-5}	1.0 to 10^8	0.127	LO
HERAPDF 1.5 LO [22]	LO	10^{-8}	1.0 to 10^9	0.13	LO
MSTW2008 LO [20]	LO	10^{-6}	1.0 to 10^9	0.13939	LO

Table 1: Specifications of the different PDF sets used. References are given in the first column.

We performed PDF set variations for Powheg and Pythia 8 separately, with the respective other generator using its default set, and simultaneously, with both generators using the same set. Information about the used PDF sets can be found in table 1. Gap fractions in the poorly described rapidity region for different choices are shown in figures 9 to 11. Varying the PDF in Powheg has a larger effect than in Pythia 8. For both generators, the effect is larger on softer jets, i.e. at the lower end of the Q_0 or Q_{sum} spectrum. Using HERAPDF 1.5 NLO in Powheg gives a relatively large deviation from the other PDFs, towards less jets and thus a slightly better description of the data. Choosing a different PDF set does not significantly improve the data/MC agreement.

Factorisation scale of PDF in Powheg Sudakov form factor. In addition to choosing a PDF set, the factorisation scale $\mu_F = Q^2$ at which the PDF is evaluated was varied in the Powheg Sudakov form factor only. By default it is the transverse momentum of the emission [9, p 84]. The default PDFs for Powheg and Pythia 8 were used. The resulting gap fractions are shown in figure 12. The effect of varying up and down by a factor of 2 is comparable in size to the spread between using different PDF sets in Powheg (figure 9), even though the scale variation is only performed in the Sudakov form factor and thus has no direct effect on the hard process. This is understandable, since the gap fractions are mostly

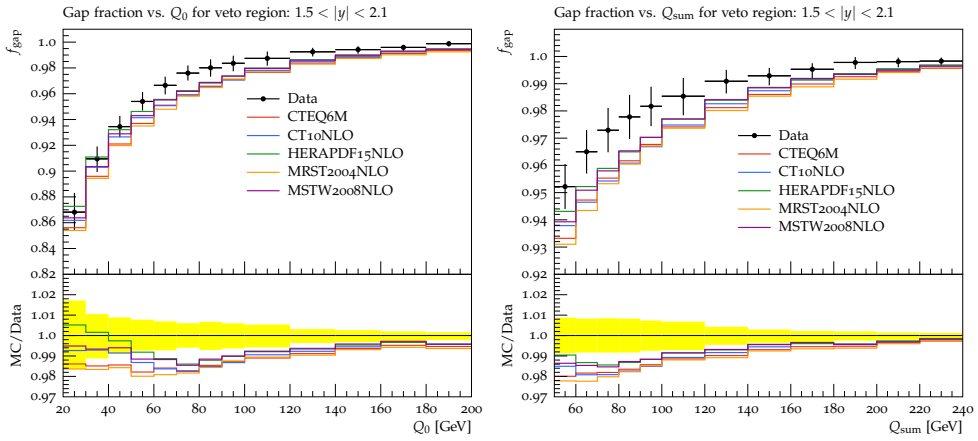

Figure 9: PDF set variations in Powheg. Pythia 8 uses default (CTEQ5L).

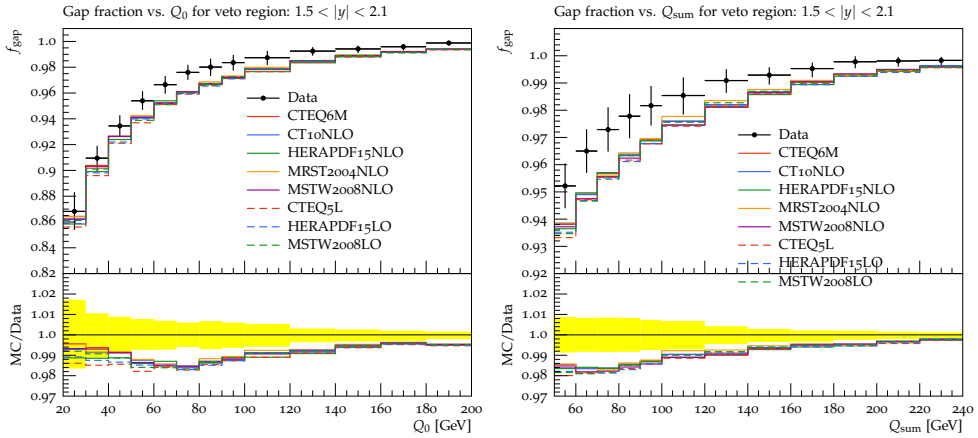

Figure 10: PDF set variations in Pythia 8. Powheg uses default (CTEQ6M).

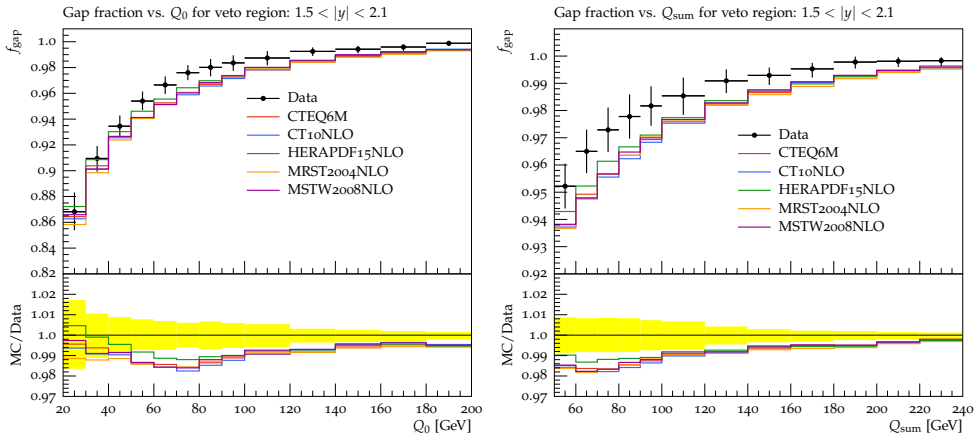

Figure 11: Simultaneous PDF set variations in Powheg and Pythia 8.

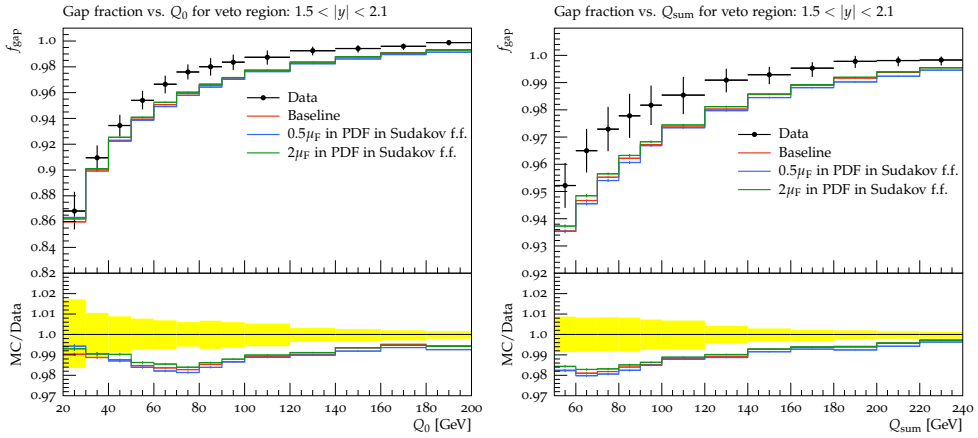

Figure 12: Variation of the PDF factorisation scale in the Powheg Sudakov form factor.

sensitive to radiation. Interestingly, figure 12 suggests that scaling μ_F up or down by 2 qualitatively has the same effect, namely to lower gap fractions. The reason is unknown, but no reason to worry given the very non-linear dependence of the Sudakov form factor on the PDFs and the complexity of the observable. Variations of the gap fractions induced by varying μ_F are too small to allow significant improvement of the modelling.

2.6 Non-description of soft wide-angle emissions

Neither the Powheg Sudakov form factor nor the parton shower describes soft wide-angle emissions of gluons very well. The reason is that the parton shower formalism is based on factorisation in the collinear limit, and not valid for wide-angle emissions. This is somewhat problematic, since they are logarithmically enhanced by softness and formally as important as hard collinear emissions, a NLL effect. The resummation in Powheg and the parton shower therefore only has leading-logarithmic accuracy everywhere, and NLL accuracy only in collinear regions of phase space.

The ratio $\mathcal{R}/\mathcal{B}$ in the Powheg Sudakov form factor does not give the correct soft wide-angle resummation in the case of more than three coloured partons. (If there are more than three, there can be multiple colour flows in the Feynman diagrams that all give the same colours to the external legs and thus interfere, complicating the situation.)

Powheg implements NLL soft-gluon resummation for processes with less than four coloured incoming and outgoing partons at leading order, but $\mathrm{t\bar{t}}$ production in hadron collisions has four coloured legs, so it does not automatically include this resummation [9, sec. 4.4]. It can be recovered in the approximation where the squared number of colours N_c^2 is considered large, as this simplifies the situation by suppressing interference effects and makes a MC description feasible [9, 23]. An approach to doing this in heavy-quark pair production such as $\mathrm{t\bar{t}}$ is discussed in reference [24]. However, this is not yet implemented in Powheg as of the writing of this report, so strictly speaking Powheg only provides LL accuracy for exclusive quantities [11].

In $\mathrm{t\bar{t}}$ events, the scale of the hard process is very high, at least 350 GeV, the mass of the top quark pair. Therefore, the argument of the logarithms L has a large numerator and even NLL effects may be sufficiently enhanced to be important. In the case of soft wide-angle emissions this means that their transverse momentum may be quite large. How hard the additional radiation in $\mathrm{t\bar{t}}$ events may be can be seen in the transverse momentum spectrum of $\mathrm{t\bar{t}}$ pairs. The cross section is not peaked sharply at $p_{\perp,\mathrm{t\bar{t}}} \approx 0$ GeV, but stays essentially the same until 60 GeV before decreasing steeply [25]. Any transverse momentum of the $\mathrm{t\bar{t}}$ system must be balanced by additional radiation, so the $p_\perp$ spectrum of the total radiation is the same as that of the $\mathrm{t\bar{t}}$ pair.

Since no MC description is available in Powheg + Pythia 8, we cannot assess directly how large the effect of including soft wide-angle emissions would be. We instead try to estimate its size by varying other NLL contributions in the Powheg Sudakov form factor, such as the strong coupling. We have shown above that changing the Powheg + Pythia 8 matching scale should introduce NLL effects, but only affecting emissions softer than the hardest—unless the scale is increased, in which case Pythia 8 can generate even harder emissions.

2.7 Strong coupling

The behaviour of the strong coupling in the Powheg Sudakov form factor was changed by the following variations:

- rescaling the renormalisation scale μ_R at which α_s is evaluated by 0.5 and 2.0,
- switching CMW rescaling on and off,

where CMW rescaling is a trick to take into account certain soft-gluon corrections to emission cross sections simply by making a particular choice for the scale at which α_s is evaluated [26]. It is necessary to be able to achieve NLL accuracy of the resummation. Both variations produce formally NLL effects, as shown in appendix B. In fact, they probably underestimate the size of NLL effects related to soft wide-angle emissions, because they affect the terms in the exponent only at the $\alpha_s^2 L^2$ (NLL & NNLL_σ) level, whereas the missing soft-wide angle terms are $\alpha_s L$ (NLL & NLL_σ). Results of the variations are

shown in figure 13. It can be seen that lowering (raising) μ_R lowers (raises) gap fractions, which is as expected. The strong coupling is stronger at lower scales, leading to emissions that tend to be more energetic and thus more jets passing the $p_\perp$-threshold of the analysis are present. Disabling CMW rescaling corresponds to increasing μ_R and thus increases gap fractions. None of the above changes to the strong coupling improves the modelling significantly.

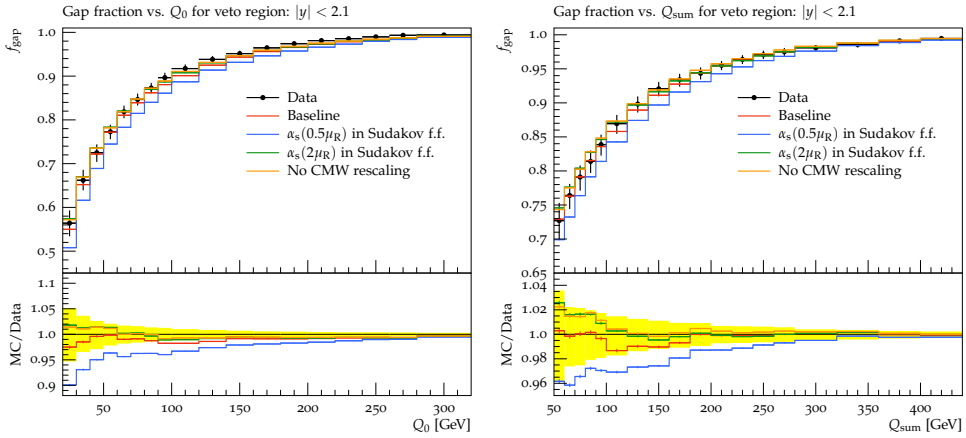

Figure 13: Rescaling the renormalisation scale at which the strong coupling is evaluated in the Powheg Sudakov form factor. Also shown is the effect of turning off CMW rescaling.

2.8 Damping resummation in Powheg

It is possible to add a damping function D taking values between 0 and 1 that limits the resummation of higher-order effects by the Sudakov form factor to below some transverse momentum scale without spoiling the NLO accuracy of the cross section. This is achieved by rescaling the real-emission cross section, $\mathcal{R} \to D\mathcal{R}$. The hardest emission cross section with damping is

$$\mathrm{d}\sigma^{(D)}_{\mathrm{pwg}} = \left[\overline{\mathcal{B}}^{(D)}\ \Delta^{(D)}_{\mathrm{pwg}}(p_\perp)\frac{\mathcal{R}(\Phi_n,\Phi_{\mathrm{rad}})}{\mathcal{B}(\Phi_m)}D(\Phi_{\mathrm{rad}}) \quad + \quad \mathcal{R}(\Phi_n,\Phi_{\mathrm{rad}})\,[1-D(\Phi_{\mathrm{rad}})]\right]\mathrm{d}\Phi_n\mathrm{d}\Phi_{\mathrm{rad}}, \tag{12}$$

where the first (second) term is the description of the hardest emission (not) including resummation of approximate higher-order corrections. They are weighted by D and $1-D$, respectively. D is constructed such that it becomes unity as the transverse momentum becomes very small, because this is where resummation is crucial and its absence would lead to a diverging cross section. On the other hand, at very large transverse momenta, Δ_{pwg} is close to one, so resummation corrections are not so important in that region of phase space. The standard choice for the damping function in Powheg is a 'washed-out step function'

$$D(\Phi_{\mathrm{rad}}) = \frac{h^2}{p_\perp^2 + h^2}, \tag{13}$$

where h is a resummation scale chosen by the user (Powheg parameter `hdamp`). The resummation scale is unphysical: it is an artefact of approximation and would not appear in an exact calculation. Therefore it may be varied within bounds that respect the approximation, with the variation giving a measure of the theory uncertainty. By default, the scale h is not set to a fixed value by the user and damping is not used ($D \equiv 1$). In this case resummation is performed up to the scale of the hard process, in our case the production of the top-antitop quark pair. This corresponds to a resummation scale of at least the energy required to produce a $\mathrm{t\bar{t}}$ pair, $2\,m_{\mathrm{top}} \approx 350$ GeV, which is very high compared to the scales at which the important resummed contributions lie. Lowering or raising it by a factor of, say, 4 should be physically acceptable. If set, h is chosen as the transverse momentum scale up to which integration in the Sudakov form factor, then denoted $\Delta^{(D)}_{\mathrm{pwg}}(p_\perp)$, is performed.

We studied the effect of changing the resummation scale h by setting it to different multiples of the top quark mass m_{top}. The results are shown in figure 14. A lower value of h (more damping) means that

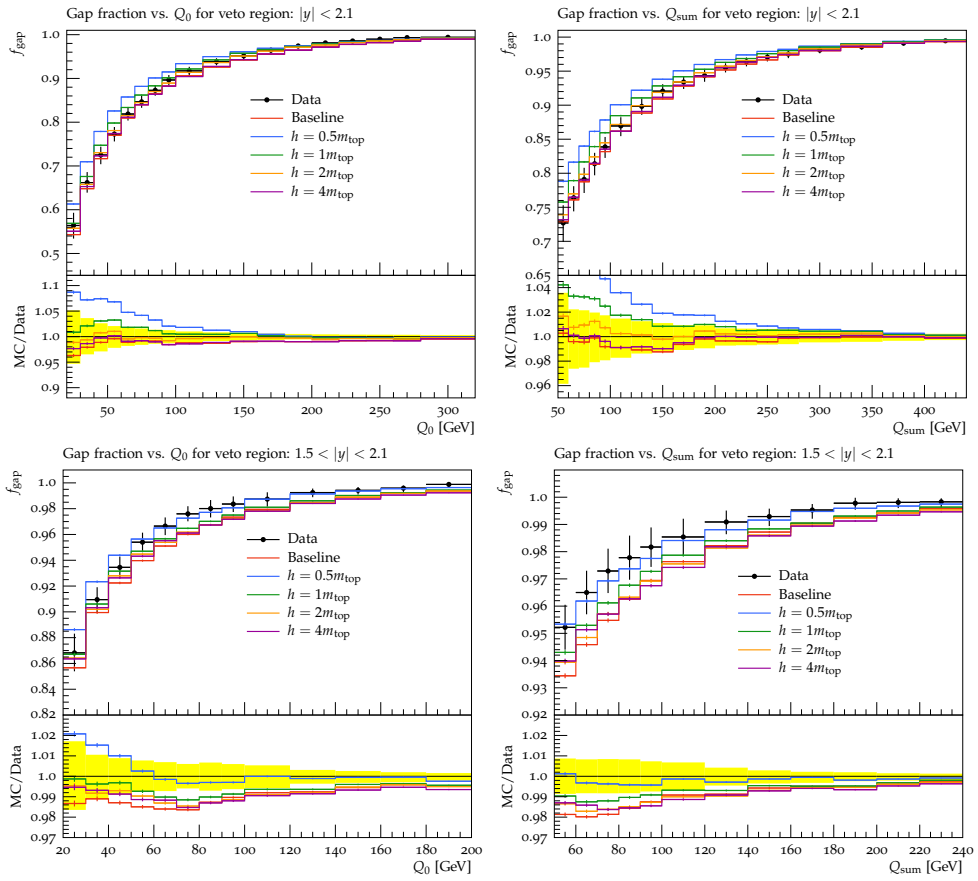

Figure 14: Damping resummation in Powheg, shown in the inclusive and the problematic rapidity region.

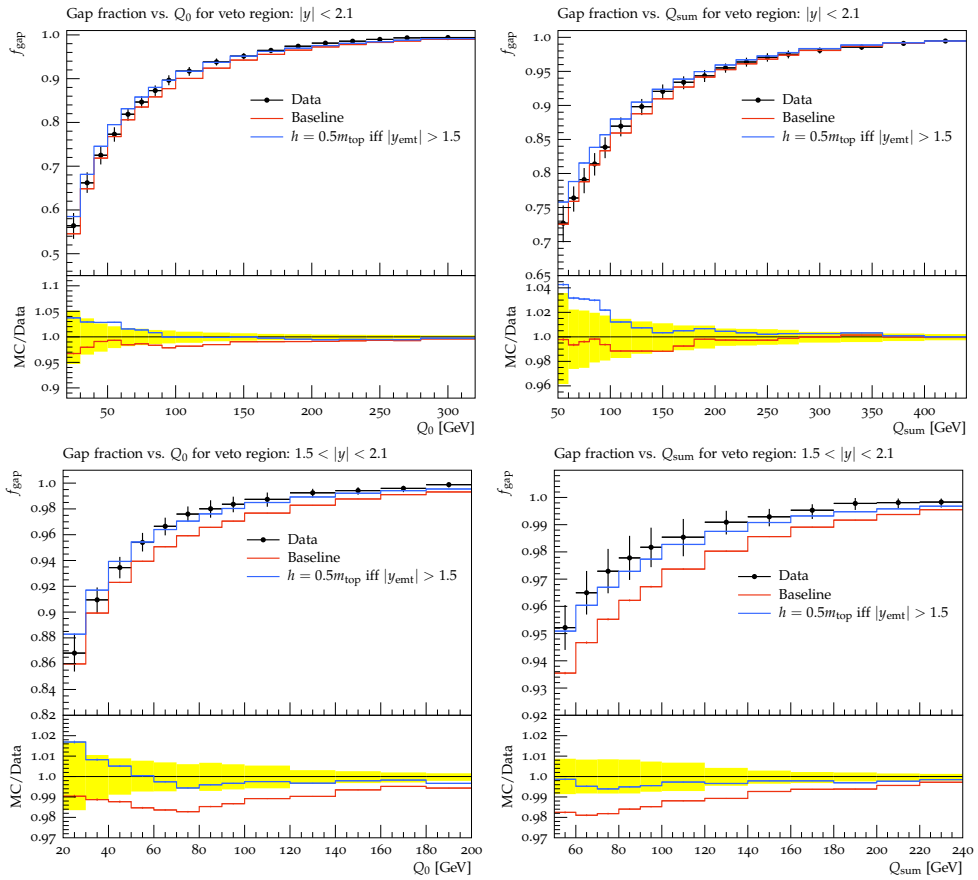

Figure 15: Damping resummation for emissions with $|y| > 1.5$ in Powheg. Agreement in the problematic rapidity region has been achieved! The agreement in the other regions suffers at low Q_0 or Q_{sum}. Of these, only the region $|y| < 2.1$ is shown, where the effect is the largest.

the hardest emission cross section is suppressed from a lower emission $p_\perp$ upwards, leading to more gaps. A higher value of h (less damping) correspondingly leads to higher gap fractions.

Variations of h between $0.5\,m_{\text{top}}$ and $4\,m_{\text{top}}$ give agreement with the data to within experimental uncertainty in all rapidity regions, but unfortunately a different value is required for good agreement in each of the regions. This leads to the idea of making the damping factor D dependent on the rapidity of the hardest emission in the laboratory frame in addition to its transverse momentum, $D(p_\perp) \to D(p_\perp, y)$. We chose to apply damping (with $h = 0.5\,m_{\text{top}}$) only if the first emission has rapidity $|y| > 1.5$. This sharp separation may be changed to a smoother transition, but we expect it to be smeared out anyway when the parton shower is attached. This removes the discrepancy in the problematic rapidity region, but somewhat worsens agreement in the other regions. However with the forward damping, agreement is (almost) within the experimental uncertainty everywhere. Figure 15 shows the gap fractions with forward damping. A slightly higher value of h somewhere between 0.5–1.0 times the top quark mass may be sufficient to improve agreement in the forward region without degrading it as much in the others.

3 Conclusions

The Monte-Carlo description of $\mathrm{t\bar{t}}$ events with additional jets at the LHC using the generator combination Powheg + Pythia 8 has been studied, focussing on the agreement of predictions with gap fractions measured by the ATLAS collaboration. Powheg alone describes gap fractions to within several percent of the data. Including a Pythia 8 parton shower can improve agreement if the matching is done carefully. Nevertheless, a data/MC discrepancy is observed in exclusive gap fractions with veto region $1.5 < |y| < 2.1$. We looked for parameter choices that improve the description. Agreement can be improved by damping resummation in Powheg for forward hardest emissions with $|y| > 1.5$ only. A slight disadvantage of this $\mathrm{t\bar{t}}$-tuned damping is that it requires some small modifications to Powheg's source code. The question remains how physically motivated introducing rapidity-dependence to the damping is. In addition, validation using other observables is needed to ensure that the tuning does not break the description elsewhere.

Most other parameter settings and scale variations were found to have a small effect on gap fractions. The same is true for the choice of PDF set. Inclusion of multiparton interactions and hadronisation has a negligible effect. The best description of the data that does not require modifications to event generators is obtained by using the default settings in Powheg and Pythia 8 as well as using Pythia 8's standard `main31` program with default settings to provide the matching. Top quark decays should be generated by Powheg.

The functionality of `main31` has been validated and documentation written for future use by the community.

All in all, it must be said that it is really astonishing how well the MC generators describe the data, considering that we are demanding agreement to within less than a percent in very exclusive and complex observables governed by QCD. Non-inclusion of the soft wide-angle emission region of phase space in both Powheg and Pythia 8 may be what limits the quality of the simulation.

I would like to thank James Monk and Thorsten Kuhl of ATLAS for the opportunity to work on this interesting project, Keith Hamilton and Emily Nurse for their excellent supervision and support, and the MCnet and ATLAS MC communities for great discussions.

References

[1] ATLAS Collaboration, *Measurement of $t\bar{t}$ production with a veto on additional central jet activity in pp collisions at $\sqrt{s} = 7$ TeV using the ATLAS detector*, Eur. Phys. J. C **72** (2012) 2043, [arXiv:1203.5015].

[2] CMS collaboration, *Measurement of jet multiplicity distributions in top quark events with two leptons in the final state at a centre-of-mass energy of 7 TeV*, CMS-PAS-TOP-12-023 (2012).

[3] CMS collaboration, *Measurement of the Jet Multiplicity in dileptonic Top Quark Pair Events at 8 TeV*, CMS-PAS-TOP-12-041 (2013).

[4] M. Cacciari, M. Czakon, M. Mangano, A. Mitov, and P. Nason, *Top-pair production at hadron colliders with next-to-next-to-leading logarithmic soft-gluon resummation*, Phys. Lett. B **710** (2012) 612–622, [arXiv:1111.5869]. Web application for calculating cross sections at http://www.lpthe.jussieu.fr/~cacciari/ttbar.

[5] R. K. Ellis, W. J. Stirling, and B. R. Webber, *QCD and Collider Physics.* Cambridge Monographs on Particle Physics, Nuclear Physics and Cosmology. Cambridge University Press, 2003.

[6] M. Cacciari, G. P. Salam, and G. Soyez, *The anti-k_t jet clustering algorithm*, JHEP **04** (2008) 063, [arXiv:0802.1189].

[7] T. Sjöstrand and P. Z. Skands, *Transverse-momentum-ordered showers and interleaved multiple interactions*, Eur. Phys. J. C **39** (2005) 129–154, [hep-ph/0408302].

[8] P. Nason, *A new method for combining NLO QCD with shower Monte Carlo algorithms*, JHEP **411** (2004) 40, [hep-ph/0409146].

[9] S. Frixione, P. Nason, and C. Oleari, *Matching NLO QCD computations with parton shower simulations: the POWHEG method*, JHEP **11** (2007).

[10] S. Alioli, P. Nason, C. Oleari, and E. Re, *A general framework for implementing NLO calculations in shower Monte Carlo programs: the POWHEG BOX*, JHEP **1006** (2010) 43, [arXiv:1002.2581].

[11] S. Frixione, P. Nason, and G. Ridolfi, *A positive-weight next-to-leading-order Monte Carlo for heavy flavour hadroproduction*, JHEP **709** (2007) 126, [arXiv:0707.3088].

[12] A. Buckley, J. Butterworth, D. Grellscheid, H. Hoeth, L. Lönnblad, J. Monk, H. Schulz, and F. Siegert, *Rivet user manual*, Comput. Phys. Commun. **184** (2013) 2803–2819, [arXiv:1003.0694].

[13] Particle Data Group, *Review of Particle Physics*, Phys. Rev. D **86** (2012).

[14] T. Sjöstrand, J. R. Christiansen, N. Desai, P. Ilten, S. Mrenna, S. Prestel, and P. Z. Skands, *PYTHIA 8 online manual*, http://home.thep.lu.se/~torbjorn/pythia81html/Welcome.html (2014).

[15] A. Buckley, J. Butterworth, S. Gieseke, D. Grellscheid, S. Höche, H. Hoeth, F. Krauss, L. Lönnblad, E. Nurse, P. Richardson, S. Schumann, M. H. Seymour, T. Sjöstrand, P. Z. Skands, and B. Webber, *General-purpose event generators for LHC physics*, arXiv:1101.2599.

[16] J. Pumplin, D. R. Stump, J. Huston, H. L. Lai, P. M. Nadolsky, and W. K. Tung, *New generation of parton distributions with uncertainties from global QCD analysis*, JHEP **207** (2002) 12, [hep-ph/0201195].

[17] H.-L. Lai, M. Guzzi, J. Huston, Z. Li, P. M. Nadolsky, J. Pumplin, and C.-P. Yuan, *New parton distributions for collider physics*, Phys. Rev. D **82** (2010) 074024, [arXiv:1007.2241].

[18] H1 and ZEUS Collaborations, *Combined measurement and QCD analysis of the inclusive $e^{\pm}p$ scattering cross sections at HERA*, JHEP **109** (2010) 1–63, [arXiv:0911.0884].

[19] A. Martin, R. Roberts, W. Stirling, and R. Thorne, *Physical gluons and high E_T jets*, Phys. Lett. B **604** (2004) 61–68, [hep-ph/0410230].

[20] A. D. Martin, W. J. Stirling, R. S. Thorne, and G. Watt, *Parton distributions for the LHC*, Eur. Phys. J. C **63** (2009) 189–285, [arXiv:0901.0002].

[21] H. L. Lai, J. Huston, S. Kuhlmann, J. Morfin, F. Olness, J. F. Owens, J. Pumplin, and W. K. Tung, *Global QCD analysis of parton structure of the nucleon: CTEQ5 parton distributions*, Eur. Phys. J. C **12** (2000) 375–392, [hep-ph/9903282].

[22] H1 and ZEUS Collaborations, *HERAPDF1.5LO PDF Set with Experimental Uncertainties*, H1prelim-13-141 and ZEUS-prel-13-003 (October, 2013).

[23] R. Bonciani, S. Catani, M. L. Mangano, and P. Nason, *Sudakov resummation of multiparton QCD cross-sections*, Phys. Lett. B **575** (2003) 268–278, [hep-ph/0307035].

[24] G. Marchesini and B. Webber, *Simulation of QCD coherence in heavy quark production and decay*, Nucl. Phys. B **330** (1990), no. 1 261–283.

[25] ATLAS Collaboration, *Measurements of top quark pair relative differential cross-sections with ATLAS in pp collisions at* $\sqrt{s} = 7$ *TeV*, Eur. Phys. J. C **73** (2013) 2261, [arXiv:1207.5644].

[26] S. Catani, B. R. Webber, and G. Marchesini, *QCD coherent branching and semi-inclusive processes at large* χ, Nucl. Phys. B **349** (1991), no. 3 635–654.

[27] ATLAS Collaboration, *Measurement of jet shapes in top-quark pair events at* $\sqrt{s} = 7$ *TeV using the ATLAS detector*, Eur. Phys. J. C **73** (2013) 2676, [arXiv:1307.5749].

[28] R. Corke and T. Sjöstrand, *Improved Parton Showers at Large Transverse Momenta*, Eur. Phys. J. C **69** (2010) 1–18, [arXiv:1003.2384].

[29] S. Alioli, *Matching Next-to-Leading-Order QCD Calculations with Shower Monte Carlo Simulations: Single Vector Boson and Higgs Boson Productions in POWHEG.* PhD thesis, Università degli Studi di Milano-Bicocca, 2009.

Appendix

A Matching Powheg and Pythia 8 using `main31`

As the Powheg emission is constructed to be the one with the highest transverse momentum, it sets a scale above which there should be no emissions. Powheg writes this upper scale to the (Les Houches event, LHE) output, into a container called `SCALUP`. If Powheg generates an emission, `SCALUP` is set to its transverse momentum. Rarely it occurs that no emission is generated by Powheg before the lower cutoff scale of the evolution is reached. In this case, `SCALUP` is set to the lower cutoff. Any emissions below `SCALUP` should be generated by the shower MC program.

The matching of Powheg-hvq and Pythia 8 is discussed in ref. [28], where it is concluded that a very high parton shower starting scale (at the kinematical limit $\sqrt{s}$, called a *power shower*) combined with vetoing of emissions harder than the one generated by Powheg is the best approach to matching the two. Such an algorithm is described in section 2.1. An implementation of the matching algorithm is in the example program `main31` included in the Pythia 8 distribution. This has become the de facto standard implementation and the name of the program almost synonymous for performing a veto-based matching of Powheg and Pythia 8. We studied the performance of `main31` and the effects of its different user configurations. When using vetoing, `main31` sets the shower starting scale to the proton-proton collision energy $\sqrt{s}$ (power shower).

The most important options that the user can choose are which transverse momentum definition to use, how to define the vetoing scale of the parton shower, and between which partons the transverse momentum associated with an emission is calculated. Shower emission vetoing can be turned off, in which case Pythia 8 returns to its default behaviour, starting the shower evolution at the Powheg scale.

Transverse momentum definition. Powheg and Pythia 8 use a different definition of transverse momentum in the generation of emissions. Consider the *squared* transverse momentum between two partons i and j. The Powheg definition[7] is

$$\left(k_\perp^{\text{pwg}}\right)^2 = d_{ij} = \left(\frac{E_i E_j}{E_i + E_j}\right)^2 2(1 - \cos\theta_{ij}), \tag{14}$$

for two partons i and j in FSR and

$$\left(k_\perp^{\text{pwg}}\right)^2 = d_{i,\pm} = E_i^2 2(1 \mp \cos\theta_i) \tag{15}$$

for an ISR parton i with respect to incoming parton $\pm$. The Powheg ISR $p_\perp$ can be obtained for the FSR one by considering $E_j \gg E_i$ and setting θ_{ij} to the angle θ_i between the emitted parton and the beam axis. It corresponds to the transverse momentum in the experimental sense. The Pythia 8 definition is

$$\left(k_\perp^{\text{py8}}\right)^2 = z^2(1-z)^2 E^2 \theta_{ij}^2, \tag{16}$$

where E is the energy of the partent parton and z the fraction of the energy E carried of by parton i in the branching. In the collinear limit $\theta_{ij} \to 0$, the two definitions agree, as can be checked easily by substituting in the parton energies $E_i = zE$ and $E_j = (1-z)E$ and expanding $\cos\theta_{ij}$ for small angles:

$$\left(k_\perp^{\text{pwg}}\right)^2 = \left(\frac{zE(1-z)E}{zE + (1-z)E}\right)^2 2(1 - \cos\theta_{ij}) \approx z^2(1-z)^2 E^2 \theta_{ij}^2 = \left(k_\perp^{\text{py8}}\right)^2. \tag{17}$$

The parton shower evolution can be constructed using either definition, since the differential cross section of collinear emissions factorises in either.

Based on the above definitions, three schemes for calculating the transverse momentum of a given branching are implemented in `main31`:

[7] See e.g. equation (3.45) in ref. [29]. Caution, other 'preliminary' definitions appear in that publication before settling on the one above.

1. Powheg ISR $p_\perp$ definition is used for both ISR and FSR
2. Powheg ISR and FSR $p_\perp$ definitions *(default)*
3. Pythia 8 $p_\perp$ definition

While choices 2 and 3 are clear enough, we are not sure how well physically motivated choice 1 is, since it calculates the transverse momentum with respect to the beam. The three choices are compared in figure 16, where it can be seen that at least choices 2 and 3 yield practically identical results.

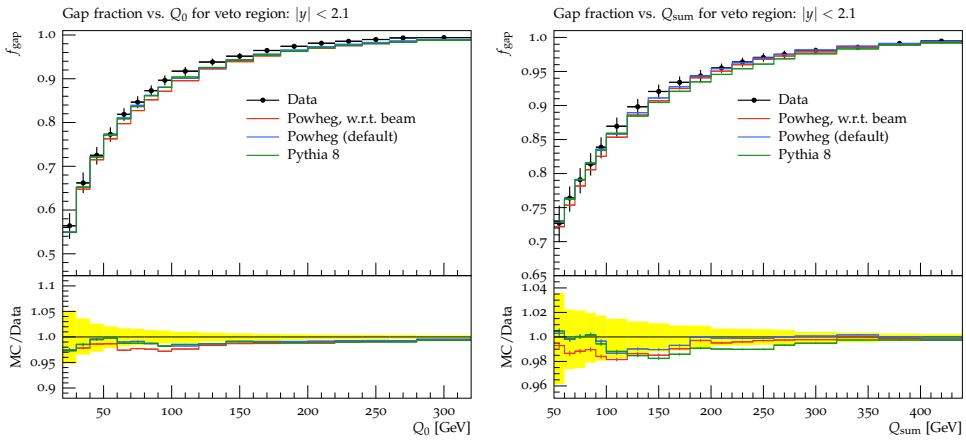

Figure 16: Different transverse momentum definitions (parameter `pTdef`).

Calculation of matching scale. Three definitions for the matching scale are implemented in `main31` for the user to choose from.

1. `SCALUP`
2. The $p_\perp$ of the Powheg emission is tested against all other incoming and outgoing partons, with the minimal value chosen
3. The $p_\perp$ of all final-state partons is tested against all other incoming and outgoing partons, with the minimal value chosen *(default)*

Gap fractions using each are shown in figure 17. The three different options lead to consecutively smaller (or equal) values for the matching scale and give less hard jets due to ISR. The most logical prescription, in the sense that it provides the best phase space coverage, would be to use `SCALUP`, but it turns out that the default choice describes the gap fraction data best.[8] Perhaps it happens to compensate for some physics not taken into account where approximations are made, such as soft wide-angle gluon radiation (section 2.6).

In events without an emission, the matching scale is always set to `SCALUP`.

Definition of transverse momentum of an emission. This definition is not about how the transverse momentum separation of two partons is calculated, but on how to select the pair of partons for which to calculate it. The alternatives are:

1. $p_\perp$ of emitted w.r.t. radiating parton *(default)*
2. The $p_\perp$ of the emission is checked against all incoming and outgoing partons, with the minimal value chosen
3. The pT of all final-state partons is tested against all other incoming and outgoing partons, with the minimal value chosen

[8] The current Pythia 8 *recommendation* is to use `SCALUP`, but this is not currently the *default* in `main31`.

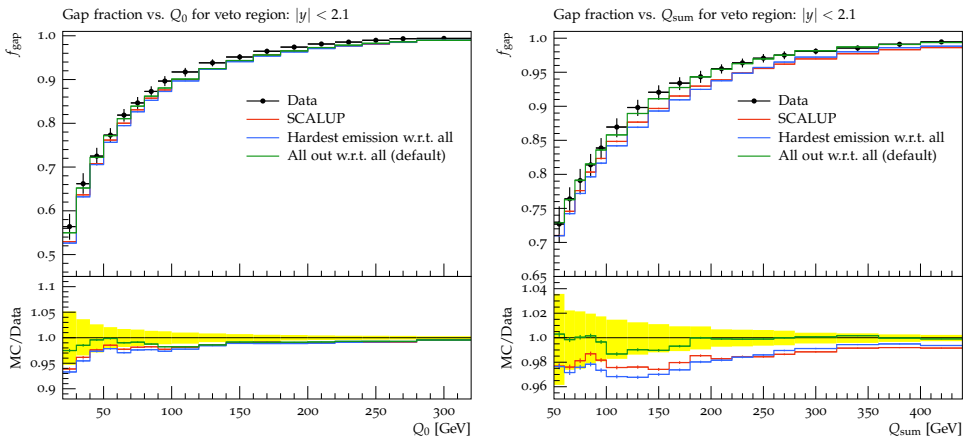

Figure 17: Different prescriptions for calculating the matching scale (parameter `pThard`).

The Pythia 8 authors warn that this setting may have a significant impact on the final distributions. The resulting gap fractions for each alternative are shown in figure 18, where it can be seen that the 2. and 3. alternative lead to too many hard emission. If the minimum $p_\perp$ of many different pairings of partons is associated with the emission, it will be smaller than or equal to the $p_\perp$ of the emitted w.r.t. the radiating parton. Hence, less emissions will be vetoed. This explains the increase in hard emissions. In alternative 3, even more pairings are formed and even more emissions pass the veto. Based on figure 18, the default choice is the only sensible one.

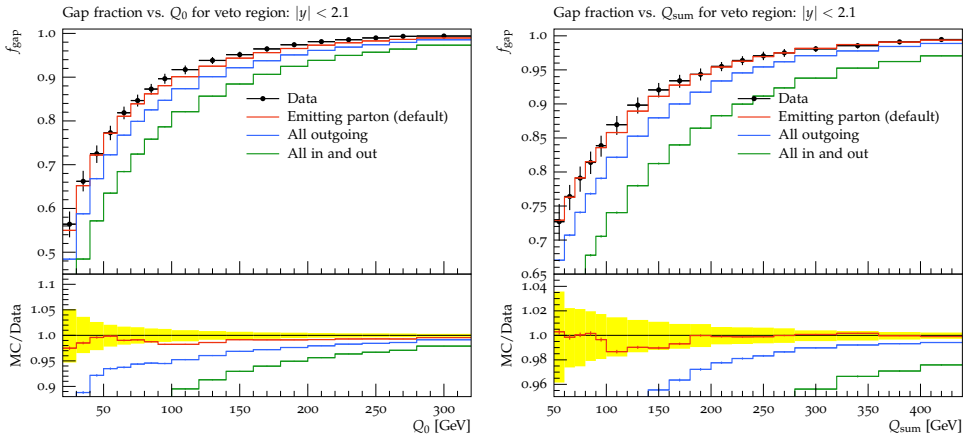

Figure 18: The transverse momentum between which particles is taken to be the scale of the emission (parameter `pTemt`).

The **parameter `vetoCount`** is the number of accepted emissions in a row after which no more vetoing is tried in the current event. We presume that its raison d'être is to speed up parton shower generation by not having to check every emission for vetoing. Contrary to what the documentation states, setting the value to 0 does not have the special meaning that all emissions are checked, but instead leads to no vetoing at all. The default value of 3 seems to be a good choice.

Although `main31` provides functionality for it, we will not discuss the **vetoing of multiparton interactions** here, for three reasons: 1) we have shown MPI to be of practically no importance to the present study (figure 6); 2) it is turned off by default in `main31`; 3) MPI take place at much lower scales than their vetoing scale, so that they are never vetoed anyway in practice.

Conclusion. We recommend using the current default settings.

B Calculations

Here we take a look at the formal orders of the effects of different scale variations.

Matching scale of Pythia 8 parton shower. Consider for example replacing the matching scale Q^2 by $2Q^2$. The Sudakov form factor changes as follows:

$$\begin{aligned}
\Delta(Q^2, p_\perp^2) \to \Delta(2Q^2, p_\perp^2) &\sim \exp \int_{p_\perp^2}^{2Q^2} \frac{dp_\perp'^2}{p_\perp'^2} \alpha_s \log\left(2Q^2/p_\perp'^2\right) \\
&\sim \exp\left\{ \int_{p_\perp^2}^{Q^2} \frac{dp_\perp'^2}{p_\perp'^2} \alpha_s \log\left(2Q^2/p_\perp'^2\right) + \int_{Q^2}^{2Q^2} \frac{dp_\perp'^2}{p_\perp'^2} \alpha_s \log\left(2Q^2/p_\perp'^2\right) \right\} \\
&\sim \exp\left\{ \int_{p_\perp^2}^{Q^2} \frac{dp_\perp'^2}{p_\perp'^2} \alpha_s \Big[\log\left(Q^2/p_\perp'^2\right) + \underbrace{\log 2}_{\sim 1} \Big] + \underbrace{\frac{\alpha_s}{2} \log^2\left(2Q^2/Q^2\right)}_{\sim \alpha_s} \right\} \\
&\sim \exp\left\{ \frac{\alpha_s}{2} \log^2\left(Q^2/p_\perp^2\right) + \alpha_s \ln\left(Q^2/p_\perp^2\right) + \alpha_s \right\}.
\end{aligned} \tag{18}$$

On the final line, the first term in the exponent is what we would get without the matching scale variation, the second is a $\alpha_s L$ term, and the last term comes from changing the upper limit of the integral. It corresponds to emissions that are neither soft nor collinear and hence not logarithmically enhanced. Therefore, we expect that only a fraction of the order of α_s of all events will have an emission harder than the Powheg emission—an 'NNLO' effect, of the same order as the probability of having one more jet. (This is an intuitive argument; we have not shown this. The only sure thing is that we can ignore it.) The largest new contribution is from the $\alpha_s L$ term, making the matching scale variation formally a NLL effect.

Renormalisation scale of α_s in Powheg Sudakov form factor. The scale dependence of α_s is, to leading order,

$$\mu^2 \frac{\partial \alpha_s}{\partial \mu^2} \approx -b\alpha_s^2, \tag{19}$$

where $b \in \mathbb{R}$ is constant. Integrating from scale μ' to scale μ gives

$$\alpha_s(\mu') \approx \alpha_s(\mu)\left[1 + \alpha_s(\mu') b \log\frac{\mu}{\mu'}\right] = \alpha_s(\mu)\left[1 + \underbrace{\alpha_s(\mu) b \log\frac{\mu}{\mu'}}_{\text{new term}}\right] + O\left(\alpha_s^3 \log(\mu/\mu')\right), \tag{20}$$

so the rescaling of μ introduces additional terms proportional to an extra power of α_s and, if we rescale by a constant real factor C of order 1 as above, a logarithm $\log C$. Schematically, the variation adds the following new terms to the integral of the Sudakov form factor:

$$\alpha_s L^2 + \alpha_s L \to \alpha_s L^2 + \alpha_s L + \alpha_s^2 L^2 + \alpha_s^2 L, \tag{21}$$

of which the additional $\alpha_s^2 L$ term is of NNLL order and thus negligible, while the $\alpha_s^2 L^2$ term is of NLL order. We conclude that the variation is a NLL effect.

Turning CMW rescaling on and off corresponds to changing μ and is thus also a NLL effect.

C Event generation and software details

Software versions

'Powheg' is `hvq` in POWHEG-BOX revision 2781 (*not* V2)

'Pythia 8' is Pythia 8.183

Rivet 2.1.0, Fastjet 3.0.3, LHAPDF 5.9.1

Custom modifications of MC generators

Capability to rescale α_s renormalisation and PDF factorisation scales, and turn off CMW rescaling

in Powheg Sudakov form factor (by Keith Hamilton)
Rapidity-dependent resummation scale (`hdamp`) variations in Powheg
Rescaling matching scale in Pythia 8